CFD and Bubble Column Reactors: Simulation and Experiment*

[a]G. M. CARTLAND GLOVER**, [a]S. C. GENERALIS**, and [a,b]N. H. THOMAS

[a]*Aston University, School of Engineering and Applied Science, Division of Chemical Engineering and Applied Chemistry, Birmingham, B4 7ET, U.K.*
e-mail: cartlgm1@aston.ac.uk, S.C.Generalis@aston.ac.uk

[b]*FRED Ltd, Aston Science Park, Birmingham B7 4JB U.K., e-mail: Nhtfred@aol.com.*

The simulation of two-phase flow in bubble columns using commercially available software from Fluent Incorporated is presented here. Data from a bubble column with a ratio of height to the column diameter of 5 : 1 are compared with simulations and experimental results for time-averaged velocity and Reynolds stress profiles are used to validate transient, two-dimensional simulations. The models are based on multiphase biological reactors with applications in the food industry. An example case of the mass transfer of oxygen through the liquid phase is also presented.

The understanding of the complexity of the fluid dynamics in bubble column reactors is very important due to its many applications in process engineering. In an attempt to enhance the performance of equipment over the past two decades many attempts have been made so that an accurate predictive model of the flow regimes present is produced.

There has been considerable development in the modelling of multiphase flows in bubble columns over the past decade. *Torvik* and *Svendsen* [1] initially modelled the flow of air bubbles through a "stagnant" liquid column (*i.e.* no liquid flow in or out of the column), though the flow was modelled using steady-state formulations for two dimensions. *Ranade* [2, 3] investigated the effect of the bubble wake models on the overall structure of bubble column flow in both two and three dimensions for steady flows. *Sokolichin, Eigenberger, Lapin*, and *Lübbert* [4—10] have been prolific in the discussion of the effects that influence the numerical solution of two-fluid and discrete particle models [9]. Their work has brought considerable influence in the techniques used to model bubble columns by including in their discussions the effects of discretization procedures [9, 10], mesh formation [5, 9, 10], mathematical phase definition, and the comparison of steady and unsteady flow models [9]. *Delnoij et al.* [11—14] developed a discrete particle model for two- [11] and three-dimensional flows [14], and discussed the effect of column height to diameter ratios [13]. This work has required validation with relevant experimental data to prove that the theory matches reality within reason. This has been difficult to achieve due to problems associated with providing enough data to compare results of simulation with those of experimentation. The turbulent nature of these flows makes it difficult to compare instantaneous profiles of variables between theoretical results and those obtained by experiment. This means that the data have to be averaged with respect to time at specific locations within the column to achieve an accurate comparison. Recently commercial software houses have incorporated the multiphase flow models which have been developed over the past ten years, into the software packages available (*e.g.* Fluent, CFX, Phoenix, ASTRID, CFDLIB). It is important to validate the software and the available models within the packages, before their use can be accepted for research and educational purposes.

THEORETICAL

The model used was developed by *Manninen et al.* [15] and incorporated in Fluent computational fluid dynamics software [16]. This model describes the flow regime as a single-phase pseudo-continuous mixture of the gaseous and liquid phases. This means that a single set of continuity and momentum equations can be used to model the flow phenomena. The momentum equation is modified to include interactions between each phase as a drift or slip velocity effect. This effect depends on the volume fraction of the dispersed and continuous phases, which is controlled by a volume

fraction equation. It is an efficient code that can predict the general flow pattern within a bubble column to reasonable accuracy.

Mathematical Model Equations

The continuity equation for the mixture phase, where $u_{m,i}$ is the mixture velocity in the i-th direction, $\partial \rho_m / \partial t$ is the partial differential for the change of the mixture density, ρ_m, with respect to time, $\partial / \partial x_i$ is the partial differential operator for the i-th direction, is as follows

$$\frac{\partial \rho_m}{\partial t} + \frac{\partial}{\partial x_i}(\rho_m u_{m,i}) = 0 \qquad (1)$$

Eqn (2) represents the momentum equation for the mixture, where on the right-hand side the forces acting on the mixture phase are collected together and include the effects of pressure $\partial p / \partial x_j$, viscous stress, gravitational acceleration in the j-th direction, g_j, momentum sources in the j-th direction, F_j, and interphase momentum interactions.

$$\frac{\partial}{\partial t}(\rho_m u_{m,j}) + \frac{\partial}{\partial x_i}(\rho_m u_{m,i} u_{m,j}) =$$
$$= -\frac{\partial p}{\partial x_j} + \frac{\partial}{\partial x_j}\mu_m\left(\frac{\partial}{\partial x_j}(u_{m,i}) + \frac{\partial}{\partial x_i}(u_{m,j})\right) +$$
$$+ \rho_m g_j + F_j + \frac{\partial}{\partial x_i}\sum_{k=1}^{n}\varphi_k \rho_k u_{D_k,i} u_{D_k,j} \qquad (2)$$

$u_{m,j}$ is the mixture velocity in the j-th direction, along with the k-th phase drift velocity, u_{D_k} in each respective direction and μ_m is the mixture phase viscosity. The volume fraction and density for each phase are represented by φ_k and ρ_k, respectively.

The volume fraction equation is used to keep a check on the volume fraction of the dispersed and continuous phases, so that estimates of the density, viscosity, and mass averaged velocity can be made through the use of eqns (4—6)

$$\frac{\partial}{\partial t}(\varphi_k \rho_k) + \frac{\partial}{\partial x_i}(\varphi_k \rho_k u_{m,i}) = -\frac{\partial}{\partial x_i}(\varphi_k \rho_k u_{D_k,i}) \quad (3)$$

The mixture density is expressed by

$$\rho_m = \sum_{k=1}^{n}\varphi_k \rho_k \qquad (4)$$

the mixture viscosity is

$$\mu_m = \sum_{k=1}^{n}\varphi_k \mu_k \qquad (5)$$

and the mass averaged velocity vector, $\boldsymbol{u}_m$, is represented by the relationship

$$\boldsymbol{u}_m = \frac{\displaystyle\sum_{k=1}^{n}\varphi_k \rho_k \boldsymbol{u}_k}{\rho_m} \qquad (6)$$

where $\boldsymbol{u}_k$ is the velocity vector for the k-th phase.

The drift and slip velocity vector equations are used to assess the interactions between the gas and liquid phases

$$\boldsymbol{u}_{D_k} = \boldsymbol{u}_k - \boldsymbol{u}_m = \boldsymbol{v}_{k,c} - \frac{1}{\rho_m}\sum_{q=1}^{n-1}\varphi_q \rho_q \boldsymbol{v}_{q,c} \qquad (7)$$

where q represents the phase index and

$$\boldsymbol{v}_{k,c} = \boldsymbol{u}_k - \boldsymbol{u}_c \qquad (8)$$

$$\boldsymbol{v}_{i,c} = \frac{(\rho_m - \rho_k)}{18\mu_c f}\left(g_j - \frac{\wp\, \boldsymbol{u}_m}{\wp\, t}\right) \qquad (9)$$

where $\boldsymbol{u}_c$ is the velocity vector for the continuous phase, $\boldsymbol{v}_{k,c}$ is the slip velocity vector between the k-th phase and the continuous phase, $\boldsymbol{v}_{i,c}$ is the slip velocity vector in the i-th direction for the continuous phase, μ_c is the continuous phase viscosity, and $\wp$ is the material derivative operator.

Friction factor, f, is used to assess the drag forces acting on the dispersed phase, as the gas bubbles move through the liquid phase, typical values of Re (Reynolds number) for the simulation are in the region $2000 < Re < 8000$

$$f = 1 + 0.05\,Re^{0.687} \quad Re < 1000 \qquad (10a)$$
$$f = 0.018\,Re \qquad Re \geqq 1000 \qquad (10b)$$

Species transport models were used to model the mass transfer of oxygen and nitrogen through the liquid domain, with the transport equation and the mass diffusion equations presented, respectively, where $w_{i'}$ is the mass fraction of species i', u_i is the i-th direction velocity, and $J_{i',i}$ is the i-th direction diffusive mass flux of species i'. $S_{i'}$ is the source term which injects the i' species into the domain, and $D_{i',m}$ is the diffusion coefficient of the i' species.

$$\frac{\partial}{\partial t}(\rho w_{i'}) + \frac{\partial}{\partial x_i}(\rho u_i w_{i'}) = -\frac{\partial}{\partial x_i}J_{i',i} + S_{i'} \qquad (11)$$

$$J_{i',i} = -\rho D_{i',m}\frac{\partial w_{i'}}{\partial x_i} \qquad (12)$$

Test Cases

To compare the theoretical model results with experimental results three cases were run using the Fluent software on a Pentium II 450 MHz processor running Windows NT. The case describes the flow phenomena for air-water bubbling beds (air density = 1.225 kg m^{-3}; water density = 998.2 kg m^{-3}; air viscosity = 1.7894×10^{-5} kg m^{-1} s^{-1}; water viscosity = 1.003×10^{-3} kg m^{-1} s^{-1}).
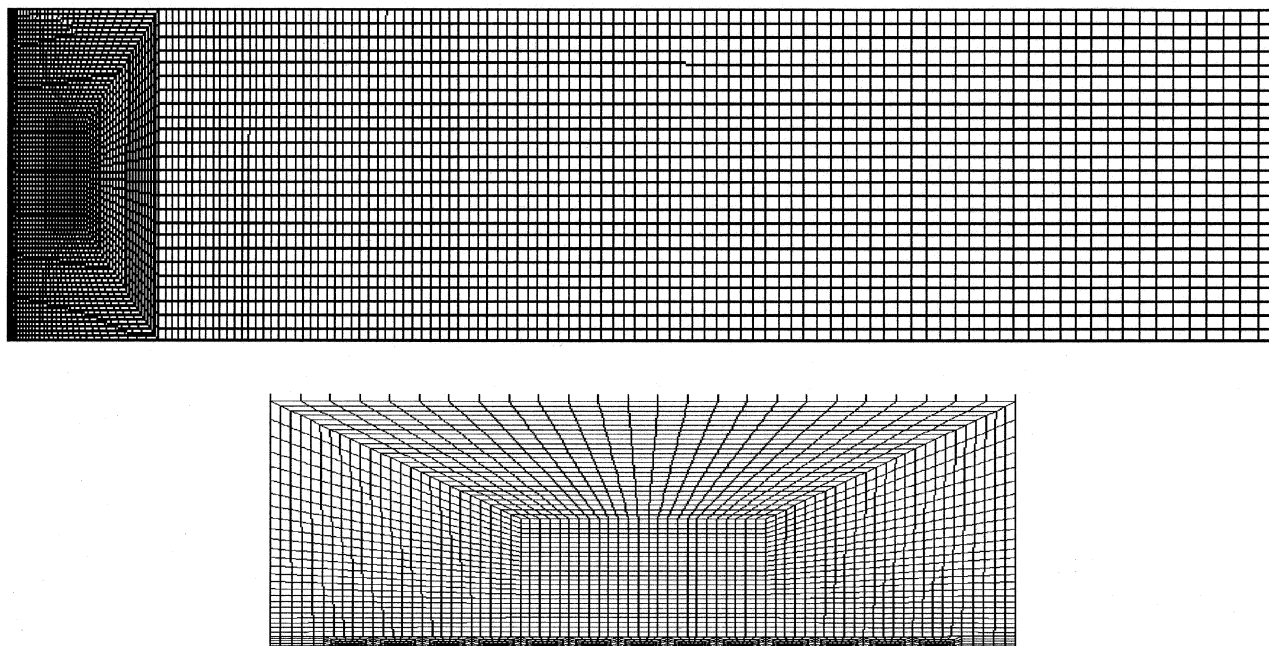
Fig. 1. The mesh for the bubble column with an aspect ratio of 5 : 1. The mesh at the top of the figure shows the whole of the column, with the base on the left-hand side of the figure. Detail of the mesh at the base of the column is shown below, both diagrams are not to scale.

The 5:1 column consisted of a distributor plate with thirteen 0.5 mm diameter inlets partially aerating the column with an overall diameter of 0.19 m. The height of the column was 1.045 m and the inlet pitch was 1.25 cm to the centre-line of each orifice. The inlets nearest to the walls were 0.02 m from the column wall. The flow boundary conditions applied to the mixture phase set the vertical gas velocity to 0.02 m s^{-1}, the gravitational acceleration to 9.81 m s^{-2}, and the bubble diameter to 5 mm. Fig. 1 shows the mesh used, this mesh contained 7325 cells, the majority of which were at the bottom of the column, in an unstructured format to reduce the number of mesh cells used.

The model used as described above is called the Algebraic Slip Mixture Model (ASMM) [15, 16]. The solver specifications for the discretization of the domain involve the following procedures, "body force weighted" for pressure, QUICK [17] for momentum, SIMPLE [18] for the velocity-pressure coupling, and a first-order discretization scheme for the volume fraction and unsteady state, laminar flow models. The under-relaxation factors, which determine how much control each of the equations has in the final solution, were set to 0.3 for the pressure, 0.7 for the momentum, 0.2 for slip velocity equations. The under-relaxation factors for the density, body forces, and volume fraction were set to 1. To assess the mass transfer of species from the gas-liquid phases, the data produced from the ASMM model were used to initialize the flow domain, and then transport of the species through the domain was assessed as a steady-state solution for a specific time.

RESULTS AND DISCUSSION

Simulations

The velocity vector field plots of the velocity magnitude in Fig. 2 present column diameter-sized vortices. The vector plots show the flow phenomena for column start-up and the instabilities in the flow mainly caused by the buoyancy flux, with vortices moving down the column. Fig. 3 shows the change of the oxygen mass transferred over a period of 60 s, when compared with the vortical structure of the flow in Fig. 2, it is observed that the concentration of oxygen is dependent on the flow regime. For the first 60 s of the simulation the majority of the mass transfer occurs at the base of the column. Fig. 4 shows the gas phase volume fraction's change with time, looking at the inlets the unstable nature of the flow is captured, even though the volume fraction is lower than the experimental results by a factor of ten. This reduction is caused by the use of a 2D-plane mesh producing lower gas flow rates when compared with the 3D column. The use of laminar flow conditions for a two-dimensional column leads to many restrictions, as the turbulent nature of the flow demands the use of a fine mesh to realize all the vortical structures in the flow, especially for the smaller eddies [10]. Though the use of the QUICK discretization method (a quadratic discretization procedure) reduces the effect of numerical diffusion associated with the use of coarse meshes and laminar flow conditions [6]. The model is limited due to the mesh being two-dimensional and therefore
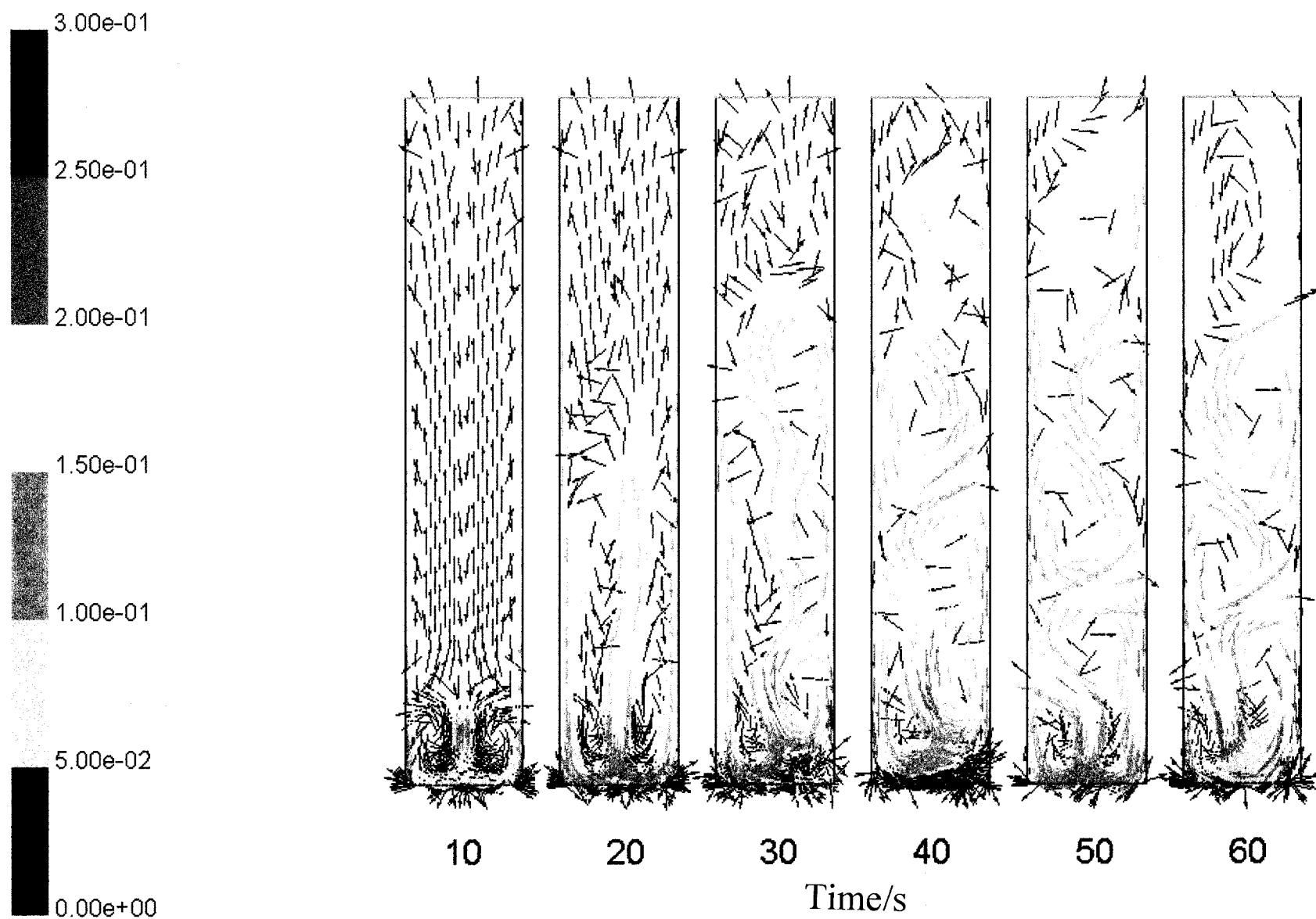
G. M. CARTLAND GLOVER, S. C. GENERALIS, N. H. THOMAS

Fig. 2. Vector fields of velocity magnitude (m s^{-1}) of the liquid phase between 10 s and 60 s of simulation time. The scale of the velocities is on the left and is between 0 m s^{-1} and 0.25 m s^{-1}.
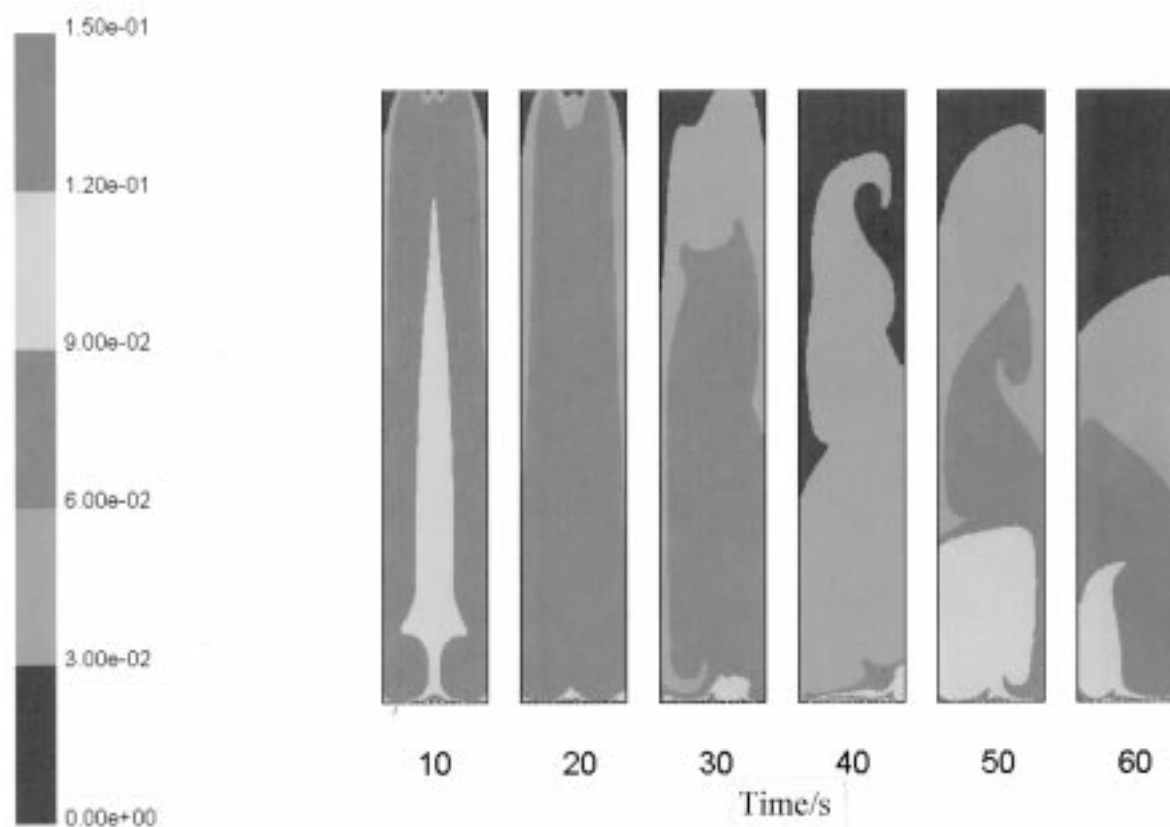
Fig. 3. Contours of the mass fraction of oxygen between 10 s and 60 s of simulation time. The scale on the left-hand side is for contours of oxygen from 0 to 0.12.

many modes of momentum transport are ignored in this model. This reduces the buoyancy flux created by the injection of the gas phase, which causes the lower gas volume fraction (Fig. 4) and velocity profile (Fig. 5). The values of the mass fraction of the oxygen component need further work and validation as only a simple mass transport case was considered to provide an example of the effect the flow field has on the transfer of oxygen to the liquid phase from an air bubble. Further investigation will need to include Henry's law, the effect of the mass transport coefficient, and the interfacial area of the bubbles to give a more representative model.

Comparison with Two-Phase Bubble Column Flow

To validate the data produced in the 5 : 1 bubble column a comparison was made with published literature. *Sanyal et al.* [16] published a comparison between the theoretical models available for use in the Fluent software and experimental results produced by Computer Automated Radioactive Particle Tracking (CARPT) with Computed Tomography (CT). The experimental data were obtained from a 0.19 m cylindrical column with a liquid height of 1.045 m for a

superficial gas velocity of 0.02 m s^{-1}, with a perforated plate distributor of 0.1 % free surface area (0.33 mm diameter holes in a square pitch). The theoretical model was based on these column specifications with a 19 by 300 mesh smooth grid. The boundary conditions applied to the column include a source term at the inlet to represent the distributor, an outlet condition, no-slip wall conditions and an axis of symmetry was applied to the column centre-line. The bubble diameter of the gas phase was set to 0.005 m for an air-water bubble column operating under atmospheric pressure. The under-relaxation factors for the pressure and momentum terms were set to 0.3 and 0.7, respectively [16].

The profiles all show good agreement with the general form time-averaged flow through the column but there is some variation in the velocity. This is due to the different boundary conditions applied. *Sanyal et al.* [16] applied a uniform source for the gas phase across the base of the column, ignoring the effect of the distributor and therefore over-estimating the volumetric flow of the gas phase. Due to the discrete sources and the two-dimensional domain, the flow regime is under-estimated when compared with the experimental flows. Fig. 6 describes the variation of the vertical liquid velocity with respect to time at a point 0.53
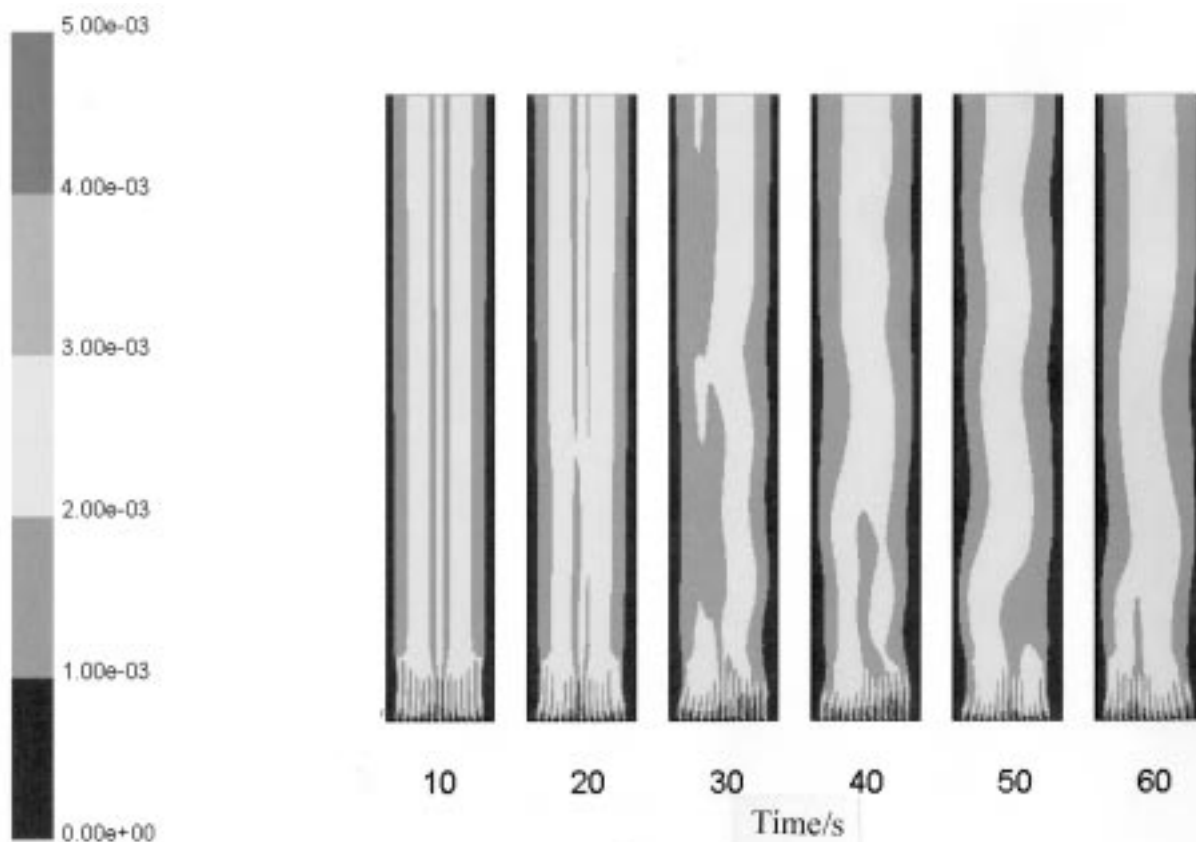
Fig. 4. Contours of the gas phase volume fraction between 10 s and 60 s of simulation time. The scale on the left-hand side is for contours of the gas phase volume fraction between 0 and 0.005.
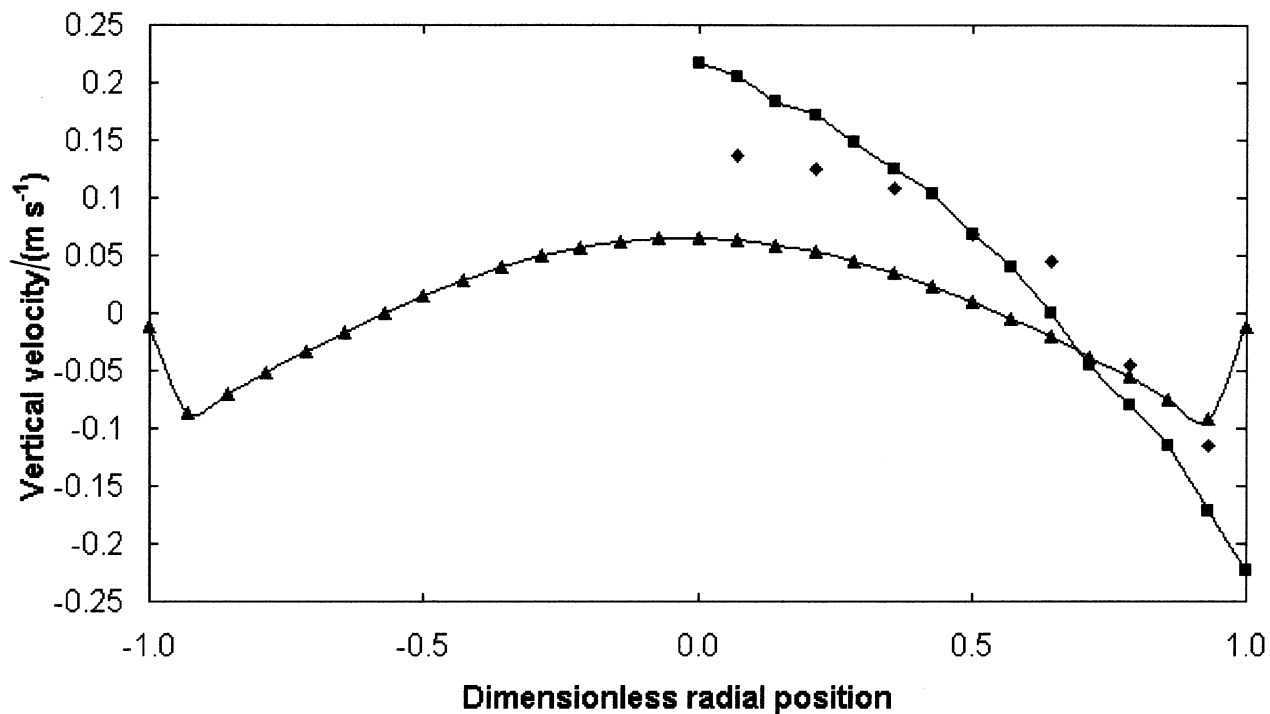

Fig. 5. The time-averaged vertical velocity profiles at a height of 0.53 m above the base of the column. ▲ *Sanyal et al.* simulated velocity profile [16]; ♦ Degaleesan experimental velocity profile [19]; ■ 2D discrete inlet mesh velocity profile.
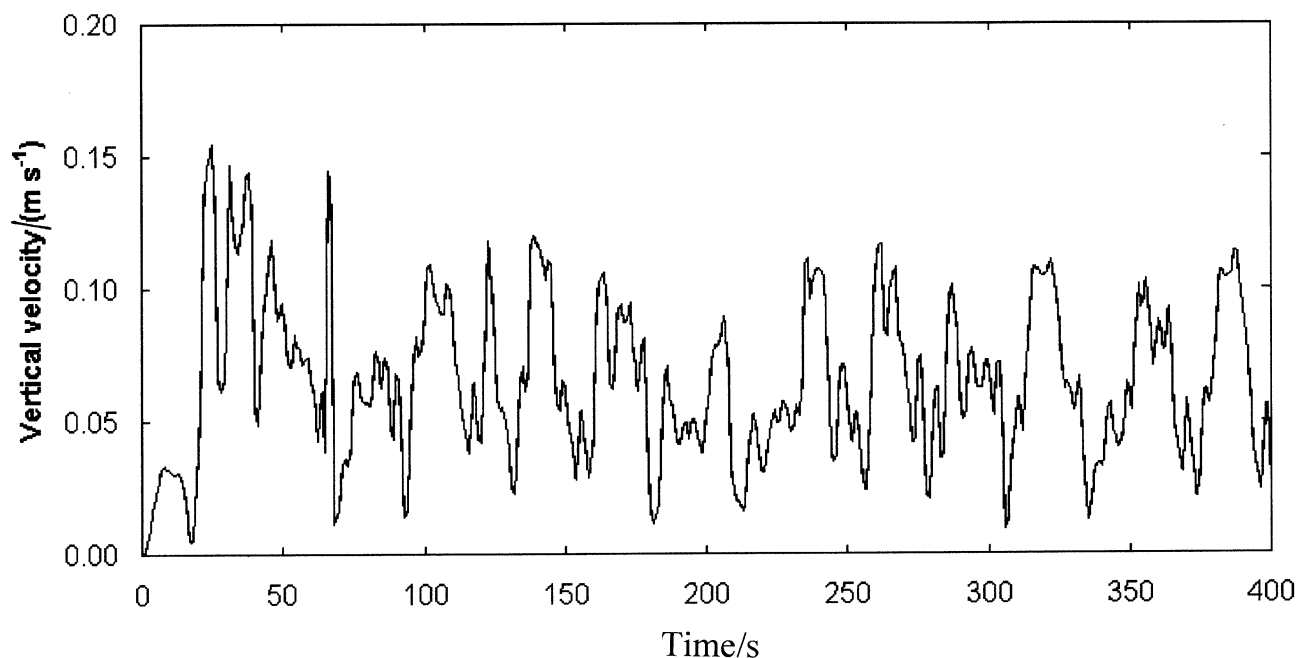
Fig. 6. Plot of the variation of the vertical velocity with time for 400 s of simulation time. The data were recorded at a point location on the column centre-line at a height of 0.53 m from the base of the column.
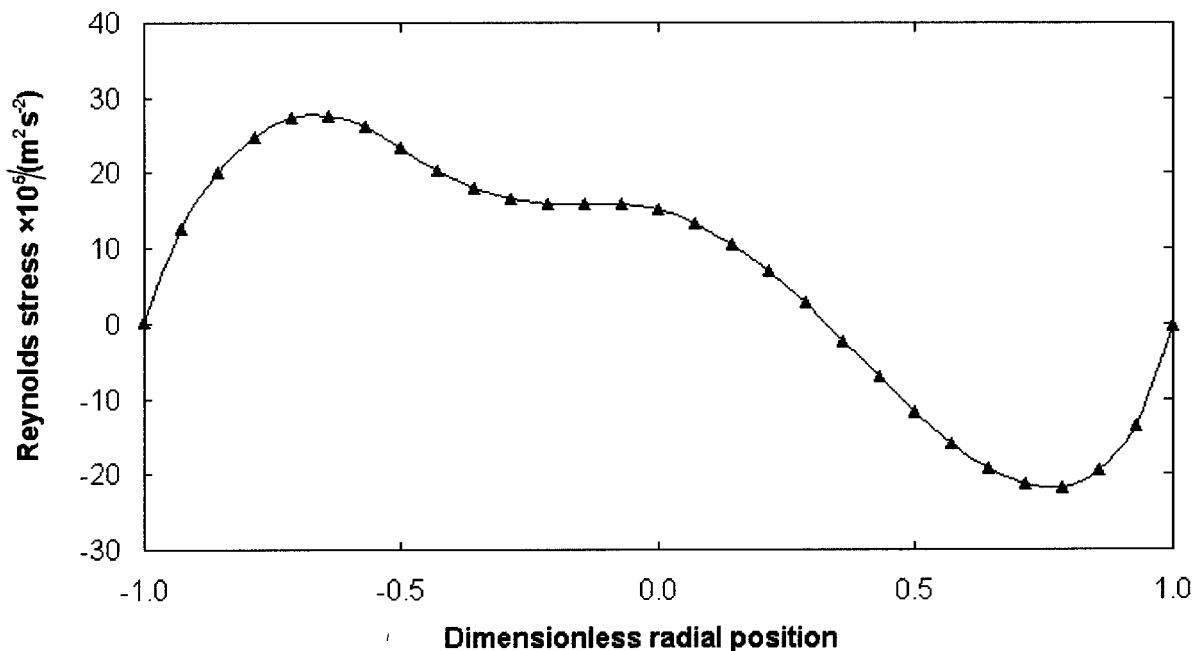

Fig. 7. The time-averaged Reynolds stress profile at a height of 0.53 m above the base of the column. ▲ $\langle u_x u_y \rangle$ profile.

m above the distributor and on the column centre-line, the curve shows that the flow is unstable with a variation of velocities between 0 and 0.16 cm s^{-1}. Longer simulation runs would show greater detail of the nature of the flow for laminar conditions, and a three-dimensional mesh of the distributor plate may provide a more representative volume fraction and velocity profile.

Reynolds Stresses

The Reynolds stress profiles presented were obtained by averaging the product of the velocity components with respect to time revealing the profiles in Figs. 7 and 8. The form of the profiles is comparable to data presented by *Mudde et al.* [20]. Fig. 7 shows the asymmetry of the flows present but the profile is pos-
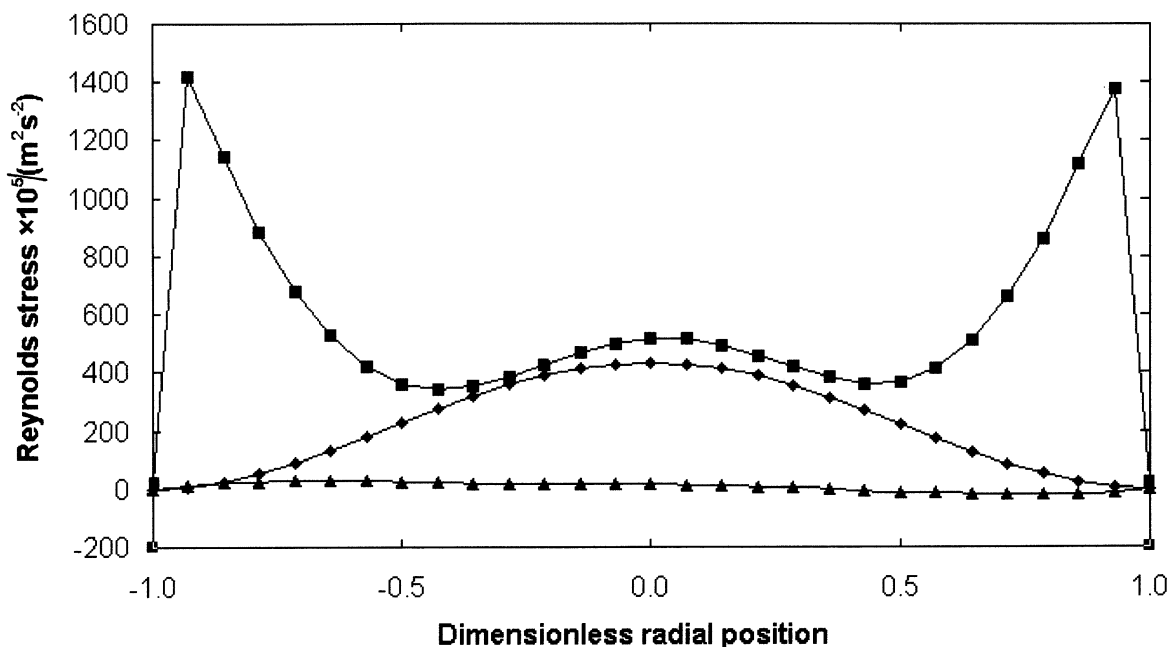
Fig. 8. The time-averaged Reynolds stresses profiles at a height of 0.53 m above the base of the column. ▲ $\langle u_x u_y \rangle$; ♦ $\langle u_x u_x \rangle$; ■ $\langle u_y u_y \rangle$.

itive then negative whereas *Mudde et al.* [20] data are negative then positive for the respective negative and positive radial positions. The forms of the $\langle u_x u_x \rangle$ ($\langle .. \rangle$ represents the time averaging of the product of the velocity vector components, the subscripts of which represent the vector directions) and $\langle u_y u_y \rangle$ profiles in Fig. 7 are also similar, but the $\langle u_y u_y \rangle$ profile has a peak in the middle of the column, this is not present for the $\langle u_y u_y \rangle$ curve of *Mudde et al.* [20]. This effect is also present in the $\langle u_x u_y \rangle$ curve as a step over the central portion of the column. The peak may be explained by the mesh configuration used to solve the domain. The change in scale between the $\langle u_y u_y \rangle$ and $\langle u_x u_y \rangle$ plots is comparable to *Mudde et al.* [20]. But the $\langle u_x u_x \rangle$ data are not, due to limitations of using a two-dimensional velocity profile (as this reduces the magnitude and the variation in the horizontal velocity) though the form of the curve is comparable to these data. The $\langle u_x u_y \rangle$ can thus be related to thermally convective flows in cavities where the profiles show a similar form [21]. This warrants further investigation with direct comparisons with thermally convective flow and two-phase bubble column flow.

CONCLUSION

The algebraic slip mixture model used to create a model of a bubble column shows good agreement that can be achieved with the symmetric form of the time-averaged velocity profiles, though the results are dependent on the mesh used to model the flow. Fig. 2 shows the asymmetric flow phenomena, which produce the symmetric profiles when the velocities are time-averaged. The differences between the case specifications cause the variance in the velocity profile presented in Fig. 5. The Reynolds stress profiles show good agreement to their form with the profiles produced by *Mudde et al.* [20], with a similar change in order of magnitude between $\langle u_x u_y \rangle$ and $\langle u_y u_y \rangle$ plots. The $\langle u_x u_y \rangle$ profile shows a form, which is similar to that of a thermally convective flow in a cavity [21]. Mass transfer of oxygen from the gas phase at the inlet shows a greater concentration at the base of the column, but the results presented do not include the diffusive effects across the liquid film where the resistance to mass transfer is a limiting factor. This limits the validity of the profiles presented and therefore further investigation of the transfer processes is required.

SYMBOLS

D	diffusion coefficient of a species	$m^2\ s^{-1}$
d	particle diameter	m
f	dimensionless friction factor	
F	external body force	$kg\ m\ s^{-2}$
g	gravitational acceleration	$m\ s^{-2}$
J	diffusive flux of a species	$kg\ m^{-2}\ s^{-1}$
w	mass fraction of a species	
p	pressure	$N\ m^{-2}$
Re	Reynolds number	
S	source term	$kg\ m^{-3}\ s^{-1}$
u	velocity	$m\ s^{-1}$

v	slip velocity	m s^{-1}
t	time	s
x	spatial coordinate	m

Reynolds Stresses

$\langle u_x u_x \rangle$	time-averaged horizontal velocity squared	m^2 s^{-2}
$\langle u_y u_y \rangle$	time-averaged vertical velocity squared	m^2 s^{-2}
$\langle u_x u_y \rangle$	time-averaged product of the vertical and horizontal velocities	m^2 s^{-2}

Greek Letters

φ	volume fraction	
μ	phase viscosity	kg m^{-1} s^{-1}
ρ	phase density	kg m^{-3}

Mathematical Operators

| ∂ | partial differential operator | |
| $\wp$ | material derivative operator | |

Subscripts and Superscripts

c	continuous phase
D_k	drift velocity of the k-th phase
i	coordinate index
i'	species index
j	coordinate index
k	phase index
m	mixture phase
n	number of phases
q	phase index
bold italic	indicates that the variable is "vectorized" or has two components for a 2D flow

REFERENCES

1. Torvik, R. and Svendsen, H. F., *Chem. Eng. Sci. 45*, 2325 (1990).
2. Ranade, V. V., *Chem. Eng. Sci. 47*, 1857 (1992).
3. Ranade, V. V., *Chem. Eng. Res. Des. 75 (A1)*, 14 (1997).
4. Becker, S., Sokolichin, A., and Eigenberger, G., *Chem. Eng. Sci. 49*, 5747 (1994).
5. Sokolichin, A. and Eigenberger, G., *Chem. Eng. Sci. 49*, 5735 (1994).
6. Lapin, A. and Lübbert, A., *Chem. Eng. Sci. 49*, 3661 (1994).
7. Devanathan, N., Duduković, M. P., Lapin, A., and Lübbert, A., *Chem. Eng. Sci. 50*, 2661 (1995).
8. Lapin, A., Lübbert, A., and Paaschen, T., *Biotechnol. Bioeng. 52*, 248 (1996).
9. Lapin, A., Lübbert, A., Sokolichin, A., and Eigenberger, G., *Chem. Eng. Sci. 52*, 611 (1997).
10. Sokolichin, A. and Eigenberger, G., *Chem. Eng. Sci. 54*, 2273 (1999).
11. Delnoij, E., Lammers, F., Kuipers, J. A. M., and van Swaaij, W. P. M., *Chem. Eng. Sci. 52*, 1429 (1997).
12. Delnoij, E., Kuipers, J. A. M., and van Swaaij, W. P. M., *Chem. Eng. Sci. 52*, 3623 (1997).
13. Delnoij, E., Kuipers, J. A. M., and van Swaaij, W. P. M., *Chem. Eng. Sci. 52*, 3759 (1997).
14. Delnoij, E., Kuipers, J. A. M., and van Swaaij, W. P. M., *Chem. Eng. Sci. 54*, 2217 (1999).
15. Manninen, M., Taivassalo, V., and Kallio, S., *VTT Publications*, p. 288. Espoo, Finland, 1996.
16. Sanyal, J., Vásquez, S., Roy, S., and Duduković, M. P., *Chem. Eng. Sci. 54*, 5071 (1999).
17. Leonard, B. P., *Comp. Meth. Appl. Mech. 19*, 59 (1979).
18. Patanakar, S. V., *Numerical Heat Transfer and Fluid Flow*. McGraw-Hill, New York, 1980.
19. Degaleesan, S., *D.Sc. Thesis*. Washington University, St. Louis, Missouri, USA, 1997.
20. Mudde, R. F., Lee, D. J., Reese, J., and Fan, L.-S., *AIChE J. 43*, 913 (1997).
21. McBain, G. D., *J. Fluid Mech. 401*, 365 (1999).